Article

Immunity

Long-Lived Plasma Cells Are Contained within the CD19^{-}CD38^{hi}CD138^{+} Subset in Human Bone Marrow

Graphical Abstract

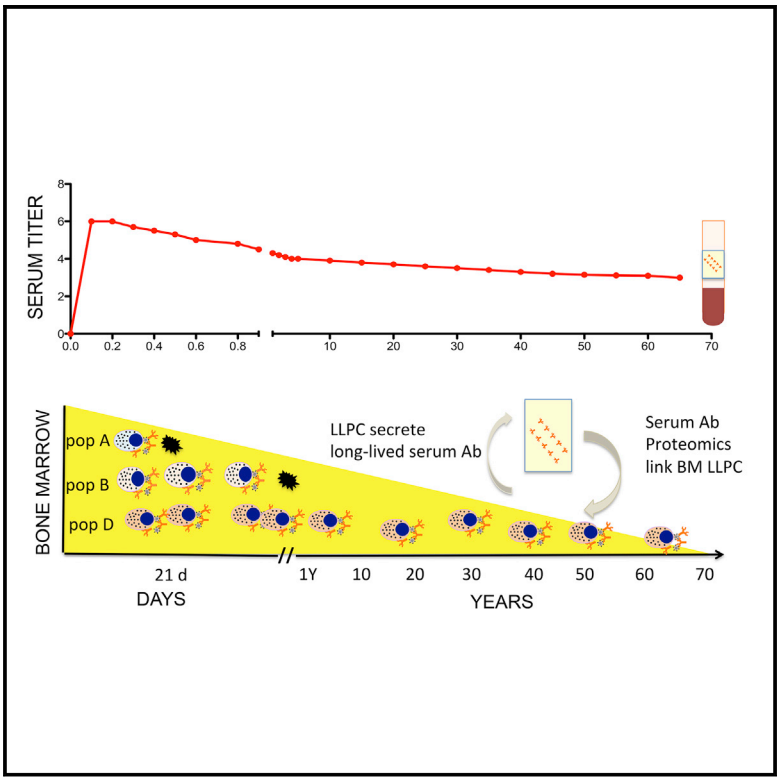

Authors

Jessica L. Halliley, Christopher M. Tipton, Jane Liesveld, ..., Wan Cheung Cheung, Iñaki Sanz, F. Eun-Hyung Lee

Correspondence

f.e.lee@emory.edu

In Brief

Anti-viral antibodies can persist in the serum for a lifetime, but their cellular origin has remained elusive. Lee and colleagues show that long-lived plasma cells (LLPCs) in human bone marrow are contained within a CD19^{-}CD38^{hi}CD138^{+} cell population, which has an uncoupled VH repertoire representing a historical record of antigenic exposure.

Highlights

- The CD19^{-}CD38^{hi}CD138^{+} BM PC subset represents human LLPCs
- CD19^{-}CD38^{hi}CD138^{+} BM LLPCs are responsible for long-lived viral antibodies in serum
- BM LLPCs have a VH repertoire that is uncoupled from other BM PC subsets
- BM LLPCs have a unique RNA transcriptome compared to other BM PC subsets

Accession Numbers

SRP057017

Halliley et al., 2015, Immunity *43*, 132–145
July 21, 2015
http://dx.doi.org/10.1016/j.immuni.2015.06.016

CellPress

CellPress

Immunity
Article

Long-Lived Plasma Cells Are Contained within the CD19^{-}CD38^{hi}CD138^{+} Subset in Human Bone Marrow

Jessica L. Halliley,[1,2] Christopher M. Tipton,[3,4] Jane Liesveld,[5] Alexander F. Rosenberg,[6] Jaime Darce,[7] Ivan V. Gregoretti,[7] Lana Popova,[7] Denise Kaminiski,[6] Christopher F. Fucile,[6] Igor Albizua,[1] Shuya Kyu,[1] Kuang-Yueh Chiang,[8] Kyle T. Bradley,[9] Richard Burack,[10] Mark Slifka,[11] Erika Hammarlund,[11] Hao Wu,[12] Liping Zhao,[12] Edward E. Walsh,[13] Ann R. Falsey,[13] Troy D. Randall,[14] Wan Cheung Cheung,[7,15] Iñaki Sanz,[3,4,16] and F. Eun-Hyung Lee[1,4,16,*]

[1]Divisions of Pulmonary, Allergy, & Critical Care Medicine, Emory University, Atlanta, GA 30322, USA
[2]Pulmonary & Critical Care Medicine, University of Rochester Medical Center, Rochester, NY 14642, USA
[3]Division of Rheumatology, Emory University, Atlanta, GA 30322, USA
[4]Lowance Center for Human Immunology in the Departments of Medicine and Pediatrics, Emory University, Atlanta, GA 30322, USA
[5]Divisions of Hematology/Oncology/James P. Wilmot Cancer Institute, University of Rochester Medical Center, Rochester, NY 14642, USA
[6]Division of Allergy, Immunology, and Rheumatology, University of Rochester Medical Center, Rochester, NY 14642, USA
[7]Cell Signaling Technology, Inc., Danvers, MA 01923, USA
[8]Department of Pediatrics, Aflac Cancer and Blood Disorders Center, Emory University, Atlanta, GA 30322, USA
[9]Department of Pathology & Laboratory Medicine, Emory University, Atlanta, GA 30322, USA
[10]Department of Pathology, University of Rochester Medical Center, Rochester, NY 14642, USA
[11]Oregon Health & Sciences University, Beaverton, OR 97006, USA
[12]Department of Biostatistics and Bioinformatics, Emory University, Atlanta, GA 30322, USA
[13]Division of Infectious Diseases, University of Rochester Medical Center & Rochester General Hospital, Rochester, NY 14621, USA
[14]Division of Clinical Immunology and Rheumatology, University of Alabama at Birmingham, Birmingham, AL 35294, USA
[15]Present address: Global Biotherapeutic Technologies, Pfizer, Cambridge, MA 02139, USA
[16]Co-senior author
*Correspondence: f.e.lee@emory.edu
http://dx.doi.org/10.1016/j.immuni.2015.06.016

SUMMARY

Antibody responses to viral infections are sustained for decades by long-lived plasma cells (LLPCs). However, LLPCs have yet to be characterized in humans. Here we used CD19, CD38, and CD138 to identify four PC subsets in human bone marrow (BM). We found that the CD19^{-}CD38^{hi}CD138^{+} subset was morphologically distinct, differentially expressed PC-associated genes, and exclusively contained PCs specific for viral antigens to which the subjects had not been exposed for more than 40 years. Protein sequences of measles- and mumps-specific circulating antibodies were encoded for by CD19^{-}CD38^{hi}CD138^{+} PCs in the BM. Finally, we found that CD19^{-}CD38^{hi}CD138^{+} PCs had a distinct RNA transcriptome signature and human immunoglobulin heavy chain (VH) repertoire that was relatively uncoupled from other BM PC subsets and probably represents the B cell response's "historical record" of antigenic exposure. Thus, our studies define human LLPCs and provide a mechanism for the life-long maintenance of anti-viral antibodies in the serum.

INTRODUCTION

Circulating high-affinity antibodies provide protection against previously encountered pathogens. This serological memory is maintained for decades by long-lived plasma cells (LLPCs) without re-exposure to antigen (Amanna et al., 2007; Fairfax et al., 2008; Oracki et al., 2010). In mice, virus-specific LLPCs survive in the bone marrow (BM) and secrete antibody for essentially the animal's lifespan (Manz et al., 1997; Slifka and Ahmed, 1998). These LLPCs are maintained in the absence of memory B cells (Ahuja et al., 2008; Slifka and Ahmed, 1998), suggesting that they are truly long-lived, rather than being replenished from memory precursors.

BM-resident LLPCs are also thought to be the main source of circulating IgG antibody in humans (McMillan et al., 1972). The striking longevity of at least some human PCs is best illustrated by the life-long persistence of serum antibodies generated in response to natural infection by measles and mumps viruses, whose half-life has been estimated at 3,014 and 542 years, respectively (Amanna et al., 2007). In contrast, serum antibody responses against tetanus vaccination have a half-life of 11 years and responses to influenza viruses are variable depending on whether exposure was by immunization or infection (Amanna et al., 2007). Such a wide range is consistent with differential participation of bona fide LLPCs in different immune responses, a proposition also supported by the differential stability of diverse autoantibody responses and their

variable susceptibility to B cell depletion therapy (Cambridge et al., 2006).

The expression of markers commonly used to define LLPCs is heterogeneous and not limited to BM PCs. Although CD138 is expressed by BM PCs (Medina et al., 2002), its expression can also be induced on PCs in short-term cultures (Huggins et al., 2007; Jourdan et al., 2011) and approximately half of the circulating PCs generated during an acute immune response also express CD138 (González-García et al., 2006; Medina et al., 2002; Qian et al., 2010), even though most of these cells are short lived. In turn, CD138-expressing PCs in the BM are heterogeneous in their expression of various markers, including CD19 and HLA-DR (Liu et al., 2012; Medina et al., 2002). Moreover, receptors important for PC homing and survival, such as CXCR4 and BCMA, also fail to distinguish between long-lived and short-lived PCs (Benson et al., 2008; Medina et al., 2002). Thus, the phenotype of human LLPCs remains undefined, and as a result, these cells have not been rigorously characterized.

Here we tested whether LLPCs could be definitively distinguished from other PCs in human BM. We found that PCs specific for viruses encountered more than 40 years prior to the study were exclusively contained within the $CD19^{-}CD38^{hi}CD138^{+}$ subset. These cells have a distinct PC morphology, are predominantly non-cycling, and express many of the gene products implicated in LLPC function, homing, and survival. We also show that the $CD19^{-}CD138^{+}CD38^{+}$ cells in the BM are the only ones to encode circulating serum antibodies specific for measles and mumps and that monoclonal antibodies reconstructed from these sequences exclusively bind to the appropriate antigens. Finally, we show that the $CD19^{-}CD138^{+}CD38^{+}$ subset of BM PCs has a distinct RNA transcriptome signature and a broadly diverse VH repertoire that is not dominated by large, clonally related populations and contains sequences that are mostly unrelated to those in other PC populations in the BM, suggesting that these cells probably represent the historical record of antigenic exposure.

RESULTS

Characterization of Distinct PC Subsets in Human BM by Frequency, Ig Secretion, Morphology, and Isotypes

To understand PC heterogeneity in the human BM, iliac crest aspirates were obtained from 14 healthy adults without a history of infection or vaccination within the previous month and cell suspensions were analyzed by flow cytometry. We initially gated on live lymphocytes lacking CD3 or CD14 expression (non-T cells, non-monocytes) or IgD-negative cells (to eliminate late transitional and naive B cells) (Figure 1A). The remaining cells were divided into $CD19^{+}$ and $CD19^{-}$ populations and subsequently characterized by the expression of CD138 and CD38 (Figure 1A) as previously described (Liu et al., 2012; Medina et al., 2002; Mei et al., 2015; Rawstron et al., 2002). Because all PCs in human BM express high amounts of CD38 (Rawstron et al., 2002), we confined our subsequent analysis to four populations: $CD19^{+}CD38^{hi}CD138^{-}$ cells (subset A), $CD19^{+}CD38^{hi}CD138^{+}$ cells (subset B), $CD19^{-}CD38^{hi}CD138^{-}$ cells (subset C), and $CD19^{-}CD38^{hi}CD138^{+}$ cells (subset D) (Figure 1A). The frequencies of all the PC subsets were validated with the use of two separate anti-CD19 monoclonal antibodies (SJ25C1 and HIB19 clones) and alternative gating strategies (Figure S1). The frequencies of each of the four populations varied between individuals (Figure 1B), but subset B was generally the largest and subset C was generally the smallest. The mean yields for subsets A, B, C, and D were 3,666 ± 4,589; 4,785 ± 7,307; 1,910 ± 2,767; and 2,848 ± 4,050 cells/ml, respectively. The average percentages of BM mononuclear cells for subsets A, B, C, and D were 0.05 ± 0.02, 0.07 ± 0.06, 0.02 ± 0.02, and 0.04 ± 0.02, respectively.

To enumerate functional PCs within each subset, we performed IgG and IgA ELISPOTs. In contrast to naive B cells ($CD19^{+}IgD^{+}CD27^{-}$), all PC subsets contained IgG- and IgA-secreting cells (Figure 1C). The frequency of IgG-secreting cells was highest in subset D and lowest in subset C (Figure 1D), whereas the frequency of IgA-secreting cells was higher in subsets A and B than in subsets C and D (Figure 1D). Only in subset D was the ratio of IgG:IgA significantly different ($p = 0.03$, $N = 6$). The combined frequencies of IgG- and IgA-secreting cells made up about 20%–35% of the input population in the ELISPOT assays (Figure 1D). The low frequency of ELISPOTs is most likely due to reduced viability or functionality of sorted PCs, because control studies showed that only 24% of IgG-secreting cells in total PBMCs were recovered after the sorting process (data not shown). In addition, contamination with non-PCs was less likely because post-sort purity was 92%–95%. Moreover, similar frequencies of ELISPOTs (19%–45% of input cells) were obtained from sorted multiple myeloma cell lines. Thus, the relatively low frequencies of ELISPOTs in our sorted subsets are likely explained by reduced viability or function and not by contamination with other cell types.

Given that PCs display characteristic morphological features, such as an eccentric oval nucleus and a prominent Golgi apparatus (Miller, 1931), we performed cytospins of cells from each subset, stained them with Wright-Giemsa, and examined 100 cells in each fraction by microscopy. Cells in each subset had distinctive features of PCs (Figure 1E). However, cells from subset D displayed unique features including a more condensed nucleus and a higher cytoplasm/nucleus ratio (Figure 1E). In addition, cells in subset D had the most homogeneous features, with consistently well-rounded nuclei and distinct Golgi. These distinct features were observed in cells from three separate patients (ages 40, 55, and 60 years). Lastly, a large majority (74%) of cells in subset D prominently displayed large vacuoles, a feature rarely observed (<1% of cells) in other subsets, including the other $CD138^{+}$ cells of subset B (Figure 1E). We also readily identified PCs with and without vacuoles (subsets D and B) in Wright-Giemsa-stained BM aspirates from healthy patients (Figure S2), suggesting that vacuoles are not artifacts of FACS sorting. Finally, none of our donors demonstrated any signs of malignancy for up to 2 years after analysis. Thus, we conclude that cytoplasmic vacuoles are a physiological feature of healthy PCs and are restricted to cells within subset D.

We next determined the relative expression of transcription factors involved in either maintaining B cell identity (PAX5) or licensing PC differentiation (BLIMP-1, XBP1). We found that PAX5 was poorly expressed in every PC subset compared to naive and memory B cells (Figure 1F), whereas BLIMP-1 and XBP1 were both highly expressed by subsets A, B, and D, but are nearly undetectable in naive and memory B cells. These

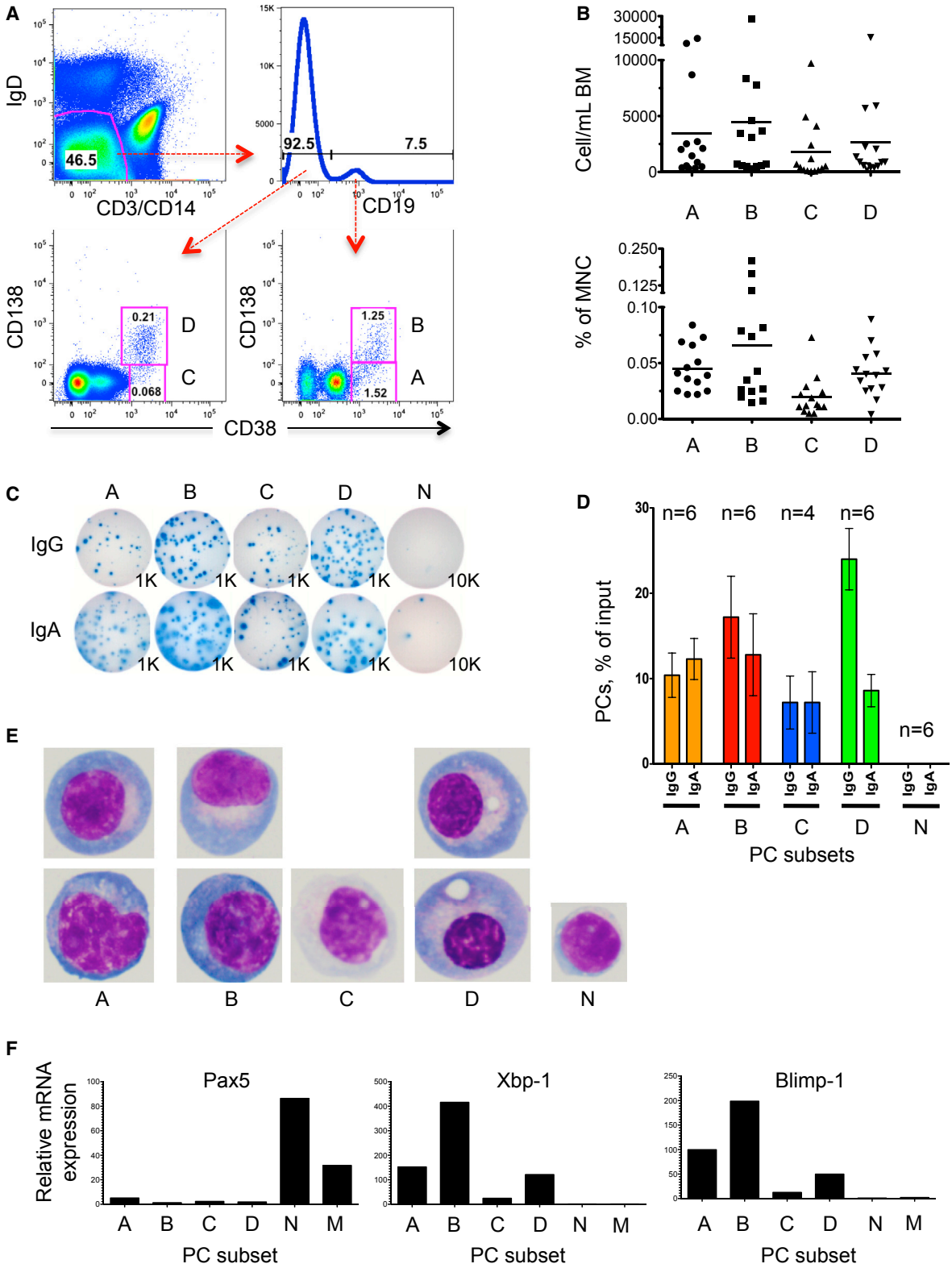

Figure 1. PC Subsets in Human BM

(A) PC subsets in the BM were sorted by excluding cells that express CD3, CD14, and IgD and separating cells into $CD19^+$ and $CD19^-$ fractions (top). Lower panels represent subsets of $CD19^-IgD^-$ (left) and $CD19^+IgD^-$ (right) fractions with PC subsets A, B, C, and D identified by CD38 and CD138. (One representative example of 31 samples analyzed.) Alternative gating strategies quantified similar frequencies of cells in each subset (Figure S1).

(legend continued on next page)

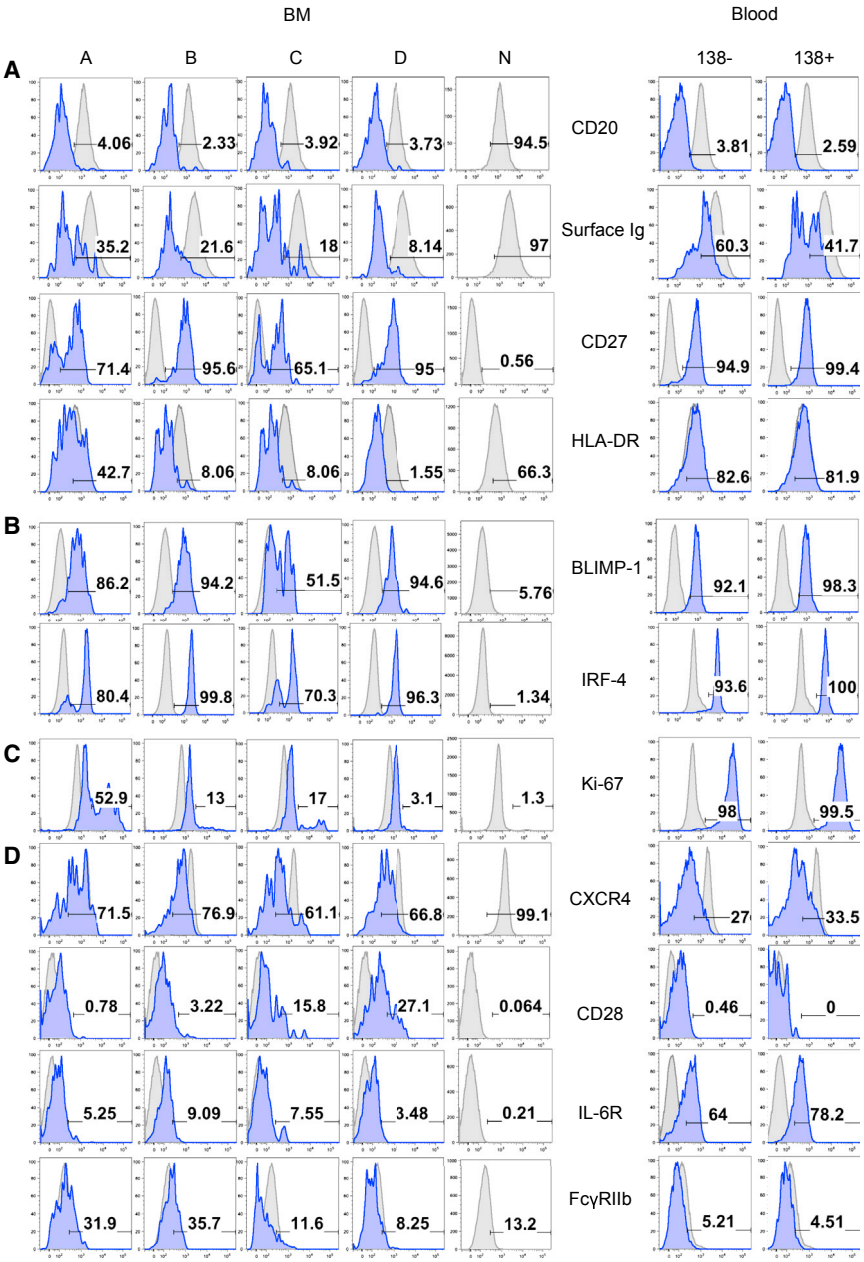

Figure 2. Characterization of BM PC Subsets and Blood Plasmablasts

Representative histograms of PC subsets A–D and naive B cells (N) in BM and peripheral blood ($CD138^-$ and $CD138^+$) plasmablasts (PBs) obtained 7 days after vaccination showing surface expression of CD20, surface Ig, CD27, and HLA-DR (A), intracellular BLIMP-1 and IRF4 (B), intracellular Ki-67 (C), and surface expression of CXCR4, CD28, IL-6R, and FcγRIIb (D). Expression on control naive B cells shown in gray. Representative number of samples for each marker shown in Table S1.

data support the contention that subsets A, B, and D are primarily composed of terminally differentiated PCs.

As B cells differentiate into PCs, they lose features of B cells (such as CD20 and surface Ig), exit cell cycle, gain expression of the transcription factor BLIMP-1, and upregulate receptors for homing and survival in the BM (Hauser et al., 2002; Tourigny et al., 2002; Turner et al., 1994). Accordingly, we used multiparameter flow cytometry to evaluate these characteristics (Figure 2; results summarized in Table S1). As shown in Figure 2A, CD20 was downregulated on nearly every cell in all four BM subsets, consistent with the loss of CD20 that begins as early as 7 days after vaccination in newly formed plasmablasts (PBs) (Qian et al., 2010). In contrast, surface Ig which is gradually downregulated during PC maturation was expressed on more than a third of the cells in subset A, to a lesser extent in subsets B and C, and on only 8% of the cells in subset D. This observation is in contrast to the high frequencies of circulating PBs that express surface Ig.

Circulating PBs as well as PCs in subsets B and D uniformly expressed high amounts of CD27, a member of the TNFR family that is upregulated during B cell activation and is linked to PC differentiation (Avery et al., 2005), whereas cells in subsets A and C had a bi-modal distribution of CD27 (Figure 2A). HLA-DR, a marker of cell activation previously shown to decrease during PC maturation (Medina et al., 2002), was expressed by the vast majority of blood PBs, but exhibited a range of expression in subset A and was nearly absent from cells in subsets B–D (Figure 2A).

We also observed nearly universal expression of BLIMP-1 in subsets A, B, and D, which validates the qPCR results and

(B) Number of cells in each PC subset per ml of BM (top) and percent of mononuclear cells from each BM aspirate (bottom). N = 14, bar represents the mean.
(C) Total IgG ELISPOTs (top) and IgA ELISPOTs from subsets A–D and naive B cells (N) from one healthy donor. Input cell numbers are indicated in right corner.
(D) Frequency of IgG- and IgA-secreting cells from subsets A–D and naive B cells by unstimulated sorted cells. Respective number of subjects listed above each subset (p value for subset D was 0.03, for other subsets A, B, C, and N were not significant [NS]). Error bars represent SD.
(E) Morphology of sorted BM PC subsets (100× magnification) by cytospins and Wright-Geimsa stain. Representative images of 100 cells of each subset A–D and naive B cells are shown. Representative of three separate BM samples. Additional images from one direct bone marrow aspirate (Figure S2).
(F) Quantitative RNA expression of 5,000 sorted cells from subsets A–D and naive (N) and memory (M) B cells. Relative mRNA expression is shown in arbitrary units normalized to GAPDH. One representative example of two experiments.

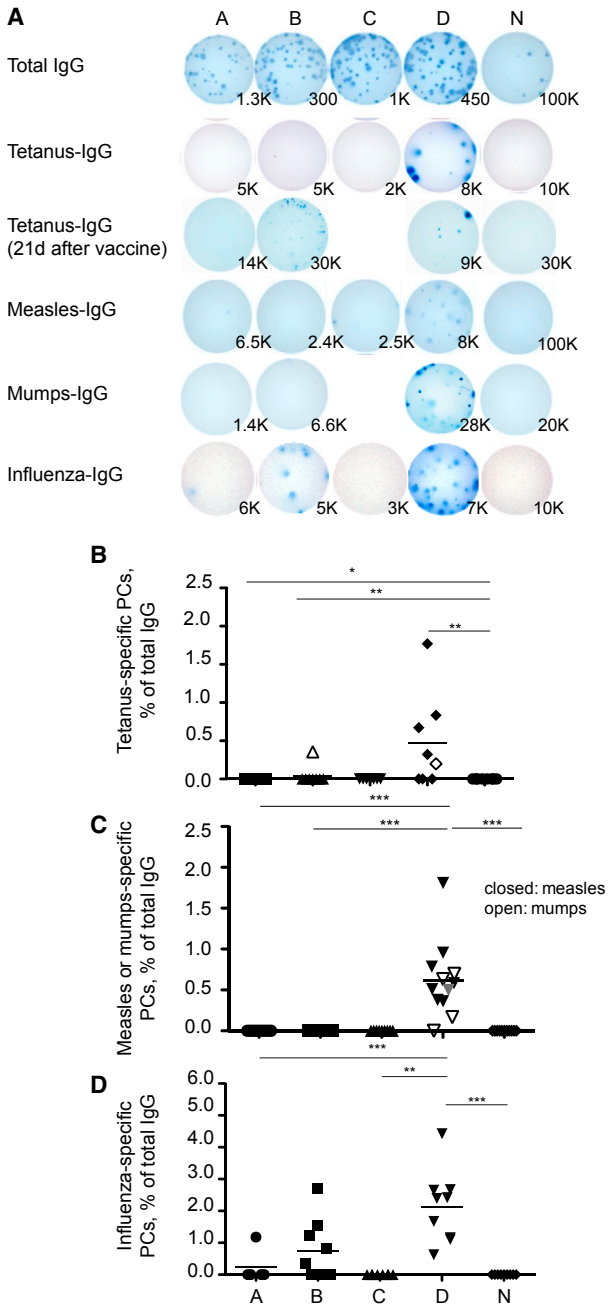

Figure 3. Identification of LLPCs by ELISPOTs

(A) ELISPOTs of total IgG-secreting cells (top row), tetanus-specific IgG-secreting cells at steady state (2nd row), tetanus-specific IgG-secreting cells 21 days after tetanus vaccination (3rd row), measles-specific IgG-secreting cells (4th row), mumps-specific IgG-secreting cells (5th row), and influenza (flu)-specific IgG-secreting cells (6th row). Input cell numbers at right corner.

(B) Frequency of tetanus-specific IgG-secreting cells in subsets A–D and naive B cells (N) from seven adults (mean age 45, range 33–55 years old) (filled symbols). Open symbols frequency of tetanus-specific IgG ASCs in subsets A–D and naive B cells 21 days after tetanus vaccination.

(C) Frequency of measles-specific (closed triangles) or mumps-specific (open triangles) IgG-secreting cells from BM PC subsets (subsets A, B, C, D), and naive (N) B cells from 11 adults (mean age 49 years; range 43–70 years). Gray triangle represents measles IgG PC frequency 1 year afterward.

(D) Frequency of influenza-specific IgG-secreting cells in subsets A–D and naive (N) B cells from nine subjects (mean age 45 years, range 30–56 years). A Fisher's exact test was then applied: *$p < 1 \times 10^{-2}$, **$p < 1 \times 10^{-3}$, ***$p < 1 \times 10^{-4}$.

further suggests that these subsets represent PC lineages (Figure 2B). In contrast, BLIMP-1 was expressed by only about half the cells in subset C (Figure 2B). Additionally, we found a consistently high amount of IRF4 expression in cells from subsets A, B, and D, but observed heterogeneous staining in subset C (Figure 2B), again suggesting that subset C consists of a mixture of PCs and non-PCs.

We also found that Ki-67, a nuclear protein associated with recent cell division, was expressed by a large fraction of cells in subset A, a lower frequency of cells in subset B, and a minority of subset D (Figure 2C). In direct contrast, nearly all post-vaccination PBs from peripheral blood expressed Ki-67, consistent with the idea that these cells were recently generated.

The relative expression of molecules involved in PC homing and survival was also highly informative (Figure 2D). For example, CXCR4, a chemokine receptor implicated in PC homing and retention in the BM (Hauser et al., 2002; Nie et al., 2004), was expressed on about 70% of cells in subsets A, B, and D, but on only about 42% of cells in subset C (Figure 2D). CD28, a co-stimulatory molecule associated with LLPC survival (Rozanski et al., 2011), was expressed at the highest frequency (20%) on BM cells in subset D and was virtually absent in blood PB. Despite the role of IL-6 in PC survival (Hilbert et al., 1995), IL-6R was mostly expressed by blood PBs and at a much lower frequency by any BM subset (Figure 2D). Finally, the expression of the inhibitory FcγRIIb, which promotes PC apoptosis (Xiang et al., 2007), was widely variable from subject to subject but was typically lower on cells in subsets C and D (Figure 2D).

Together, these results demonstrate that, in contrast to other BM PC subsets, cells in subset D have a uniform gene expression pattern that is consistent with the expected features of LLPCs.

Identification of Human LLPCs in the $CD19^{-}CD38^{hi}CD138^{+}$ Subset

Serum antibody responses against vaccination or infection can last for decades (Amanna et al., 2007), suggesting similar longevity for LLPCs. To test whether LLPCs were confined to a discrete population in the BM, we sorted cells from each PC subset from seven healthy adults (mean age 45 years, range 33–55 years) and performed ELISPOTs using plates coated with tetanus or with anti-IgG to enumerate all IgG-secreting cells (Lee et al., 2011). We found that tetanus-specific responses were present in subset D in only four subjects (Figures 3A and 3B), with a mean frequency of 0.51% of total IgG ASCs (range 0%–1.8%). Variability of cell numbers of the PC subsets A, B, C, and D for each individual was common and thus, to account for different cell numbers in each well, a Fisher's exact test was applied to evaluate the null hypothesis that the frequencies are equal in the two subsets. Comparisons between subsets A and D and subsets B and D are shown to be statistically different (Figure 3B) but there was no statistical difference between subsets C and D due to low cell numbers. Cell recovery from subset

C was often lowest of all BM subsets due to low frequencies (Figure 1B) and heterogeneity of this population (not all cells were PCs; Figure 2B). Thus, we concluded that long-lived responses reside predominantly in subset D.

To understand the BM PC response after a recent tetanus vaccination, we enumerated tetanus-specific IgG ELISPOTs after vaccination on days 0, 7, and 21 in the blood and on day 21 in the BM. We found no tetanus-specific ASCs in the blood prior to vaccination, but observed 76 ASCs per 10^6 PBMCs on day 7, which declined to 0 on day 21. In contrast, we observed tetanus-specific IgG ELISPOTs on day 21 in the BM in both subsets B (0.36% of total IgG) and D (0.20% of total IgG) (Figures 3A and 3B), suggesting that these subsets can be rapidly populated with ASCs after vaccination but that PCs are maintained for longer periods in subset D.

To conclusively establish the longevity of PCs in subset D, we obtained BM aspirates from 11 older healthy adults (mean age 49 years; range 43–70 years) with a high serum antibody titer to either measles or mumps and no history of MMR vaccination to ensure exposure of these viruses by natural childhood infection. We sorted cells from each of the PC subsets in the BM and performed measles-specific and mumps-specific ELISPOTs. Similar to what we observed with tetanus responses, measles-specific and mumps-specific ELISPOTs were found prominently in subset D, with a mean frequency of 0.6% (range 0%–1.8%) of total IgG ASCs (Figures 3A and 3C). Comparisons between subsets A and D (p value of 8.094×10^{-5}) and between A and B (p value of 3.06×10^{-12}) were found to be highly significant. Again, due to low cell numbers, comparison between subsets C and D was not significant. Strikingly, measles-specific ELISPOT analysis repeated a year later in one subject confirmed the restriction of the response to subset D, with nearly identical frequencies (0.6% and 0.5% of total IgG ASCs; Figure 3C). Although we could not discriminate difference between subsets D and C due to overall low cell numbers in subsets C, we conclude that the LLPCs reside in subset D because nearly all PCs in the BM reside in subsets A, B, and D.

In contrast to measles and mumps, healthy adults typically encounter influenza virus antigens annually either through vaccination or natural infection. Thus, we postulated that influenza-specific ASCs, including long-lived PCs elicited by natural infection and recently generated, short-lived PCs, will likely be distributed between multiple subsets (Skowronski et al., 2008; Yu et al., 2008). To test this possibility, we sorted PC subsets from BM aspirates from nine subjects (mean age 45 years, range 30–56 years) and performed influenza-specific ELISPOTs using the 2010 seasonal vaccine (Halliley et al., 2010; Kyu et al., 2009). We observed influenza-specific PCs in subsets A, B, and D (Figures 3A and 3D). Statistical comparisons showed differences between subsets A and D and subsets C and D but no differences between subsets B and D. Together, these results indicate that short-lived PCs can reside in subset B and possibly in subset A, whereas LLPCs are restricted to subset D.

Long-Lived Serum Antibody Responses Are Maintained by $CD19^{-}CD38^{hi}CD138^{+}$ Cells

Because the half-life of human serum IgG is 15–30 days (Morell et al., 1970), any measles-specific or mumps-specific circulating IgG present in adults who have not encountered these antigens since childhood must be recently produced by LLPCs. To formally demonstrate the cellular origin of long-lived anti-viral antibodies, we performed a coordinated analysis of serum and bone marrow of one 64-year-old adult who had been infected with measles and mumps as a child. Virus-specific IgG was affinity purified using measles or mumps antigens and interrogated by serum Ig proteomic methods described previously (Cheung et al., 2012; Sato et al., 2012). Virus-specific IgG antibodies were eluted, verified for measles or mumps activity by antigen-specific ELISA (Figure 4A), then digested and analyzed on the liquid chromatography-mass spectrometry/mass spectrometry (LC-MS/MS) (Figure 4B). Mass spectra identified from each digested eluate were compared using SEQUEST to HCDR3 sequence databases (VH1-VH6), generated from cells in subsets A, B, and D and naive B cells. Top candidate HCDR3 sequences (VKGGNLLGIRPFDS for measles and AKMIGSSAWYPFDY for mumps; Figure 4B) were identified based on the mapping of high-confidence peptide spectra. A total of 55 (measles) and 67 (mumps) peptides were mapped, covering 100% of the variable region of the gamma chains. Importantly, the unique measles and mumps HCDR3 peptide sequences were restricted to RNA sequences present only in subset D (117 VH sequences containing measles-specific HCDR3 and 59 VH sequences containing mumps-specific HCDR3; Figure 4C). These virus-specific HCDR3 sequences were not found in subsets A or B or in naive B cells (Figure 4C).

We also mapped the VL peptides digested from the mumps-specific Abs and reconstructed the most confident full-length VL-region sequences (Cheung et al., 2012; Sato et al., 2012). Using full-length heavy and light chain sequences (HCDR3: AKMIGSSAWYPFDY and LCDR3: GTWDSSLGIVL), we constructed and expressed a recombinant monoclonal antibody (Cheung et al., 2012; Sato et al., 2012) and tested its specificity by ELISA. We found that the reconstructed monoclonal antibody was specific for mumps but did not recognize measles antigens (Figure 4D). Together, these data demonstrate that LLPCs currently producing serum antibodies specific for antigens encountered decades previously originate only from subset D of the human BM.

LLPCs Have a Distinct VH Repertoire that Is Uncoupled from Other PC Subsets

The antibody repertoires expressed by different PC subsets were analyzed by NGS of sorted BM populations (subset C was not included due to low cell numbers). Consistent with our ELISPOT data (Figure 1C), subset D was differentiated by a predominant expression of IgG sequences (76%). In contrast, IgG was lower than IgA in subset A (35% and 65%) and more evenly split in subset B (56% and 44%). Despite wide variability between subjects, the average number of somatic mutations was similar in each of the BM PC subsets (21.6 ± 9.9 in A, 21.8 ± 10.0 in B, and 17.8 ± 9.3 in D).

Repertoire diversity within the different subsets was ascertained using several metrics of clonality. Unique clonotypes were comprised of all the sequences sharing the same V-D-J rearrangement and had a HCDR3 of identical length, with at least 70% sequence similarity within that region and conservation of the VH-D and D-JH junctional sequences. Of the 5,719 sequences obtained from PCs in subset A, we identified 1,037

A

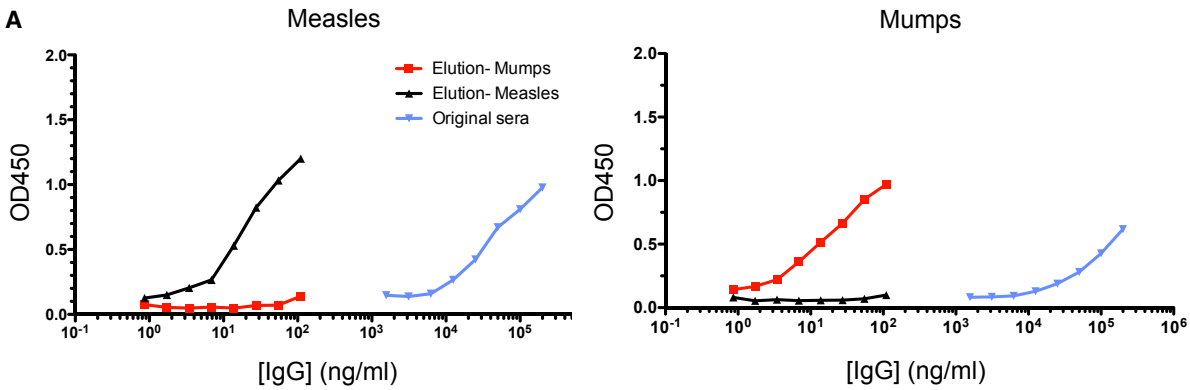

B

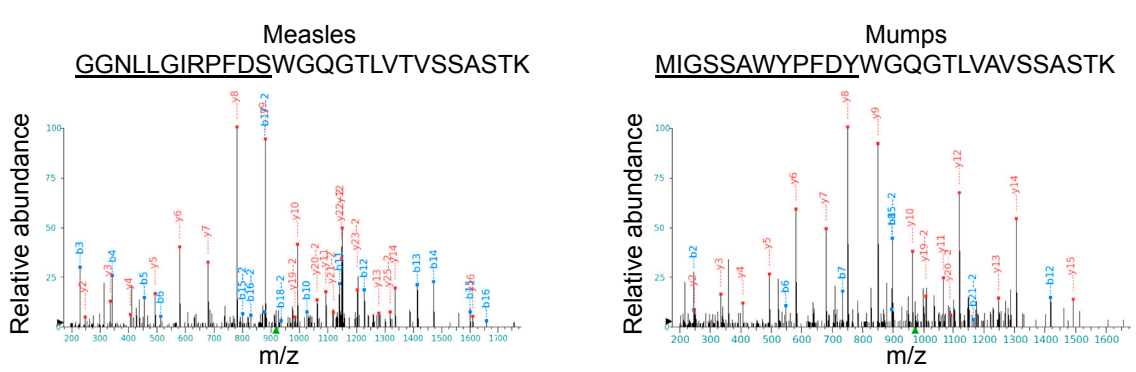

C

	A	B	C	D	N	% V region coverage	VDJ
Measles VKGGNLLGIRPFDS	0	0	ND	117	0	100	V3-9 J4D 3-10
Mumps AKMIGSSAWYPFDY	0	0	ND	59	0	100	V3-23 J4 D6-9

D

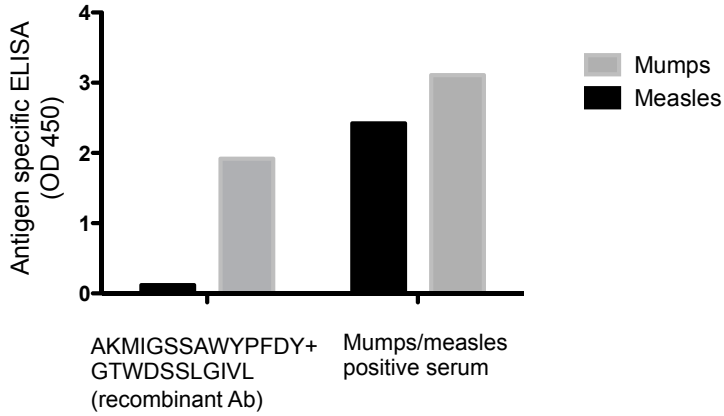

(legend on next page)

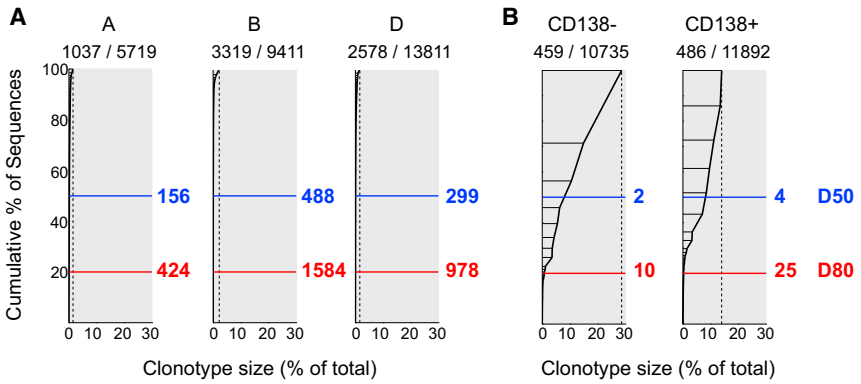

Figure 5. Clonal Diversity of BM PC Subsets and Blood PBs

The VH repertoire for VH families 1–6 was determined by next generation sequencing of cells in (A) BM subsets A, B, and D and (B) CD138$^+$ and CD138$^-$ PBs in peripheral blood after tetanus vaccination. The cumulative percentage of sequences (y axis) versus lineage (clonal) size (x axis) ranked by abundance. D50 designates the number of clonotypes in the top 50% of the sequences and D80 represents the number of clonotypes in the top 80% of the sequences. Numbers above each plot indicate frequency of unique IgG clonotypes per total number of IgG sequences.

clonotypes; of the 9,411 sequences from subset B, we identified 3,319 clonotypes; and of the 13,811 sequences from subset D, we identified 2,578 clonotypes (Figure 5A). We also found that PCs in all three subsets expressed a very diverse repertoire that was primarily composed of singletons and clonotypes of relatively small size. Specifically, the most abundant clonotype in each subset made up only 1.5% of total sequences in subset A, 2.2% in B, and 1.6% in D. A high degree of diversity within all the BM PC subsets was also indicated by very high D50 and D80 scores (representing the number of clonotypes accounting for the top 50% or 80%, respectively) of sequences within a given population. Thus, the D50 scores for subsets A, B, and D were 156, 488, and 299, respectively, and the D80 scores were 424, 1,545, and 978, respectively (Figure 5A).

As a comparative counterpoint of oligoclonal PB populations (Qian et al., 2010; Wrammert et al., 2008), we analyzed CD138$^+$ and CD138$^-$ PBs sorted from healthy subjects 7 days after tetanus vaccination and sequenced the productively rearranged VH genes from cells that had switched to either IgG or IgA. Sequences from CD138$^-$ PBs were comprised of 57% IgG and 43% IgA, whereas sequences from CD138$^+$ PBs were comprised of 63% IgG and 37% IgA. Of the 10,735 sequences from CD138$^-$ PBs, we identified 459 clonotypes, and of the 11,892 sequences from CD138$^+$ PBs, we identified 486 clonotypes (Figure 5B). The most abundant single clonotype in CD138$^-$ PBs made up nearly 30% of the total sequences (Figure 5B), whereas the most frequent clonotype in the CD138$^+$ PBs made up nearly 14% of the total sequences. Moreover, the D50 scores of CD138$^-$ and CD138$^+$ PBs were 2 and 4, respectively, whereas the D80 scores of CD138$^-$ and CD138$^+$ PBs were 10 and 25, respectively (Figure 5B). Thus, unlike the PCs in the BM, the acutely circulating PB subsets are dominated by a very small number of substantially expanded clones.

A separate LLPC compartment that contains unique antibody responses would be expected to express a repertoire that is distinct from other PC populations. Thus, we determined the degree of inter-relatedness of the PCs in subsets A, B, and D. As illustrated by Circos plots (Figures 6A and 6B) for IgG and IgA sequences, a large fraction of subset D was indeed uncoupled from other BM populations. However, subset D shared 6% of IgG and 11% of IgA clonotypes with subset A and 15% of IgG and 16% of IgA with subset B (Figures 6A and 6B). Thus, a relatively small segment of subset D sequences was shared with subsets A and B. In contrast, the repertoires of post-vaccination blood CD138$^+$ and CD138$^-$ PBs were highly connected, as shown by the fact that they shared 58% and 41% of IgG and IgA sequences, respectively (Figures 6C and 6D).

Given the polyclonality of subset D and in order to correct for sampling efficiency, we performed a control experiment by splitting 20,000 cells sorted from subset D into two fractions of 10,000 cells each and sequencing them in separate reactions. We found that only 44% of all sequences and 40% of the lineages were concordant between the two theoretically identical populations, a result consistent with a very polyclonal compartment and small average clone sizes. After applying a correction factor generated from these data, we conclude that the corrected level of repertoire connectivity between subsets D and A is 13% for IgG and 25% for IgA, and the corrected level of repertoire connectivity between subsets D and B is 34% for IgG and 36% for IgA. This result is in sharp contrast with the degree of connectivity between subsets A and B (43% of IgG and 30% of IgA prior to correction). Therefore, the application of the same correction factor would indicate almost complete identity between subsets A and B. Correction factors are at best estimates to distinguish polyclonal versus oligoclonal repertoires. In all, PC subsets in the BM are highly polyclonal with subset D

Figure 4. Serum Antibodies to Measles and Mumps Restricted to BM Subset D

(A) ELISA activity of affinity-purified measles-specific and mumps-specific serum antibodies from a 64-year-old adult. Original sera (blue), measles eluted fraction (red), and mumps eluted fraction (black) are shown.

(B) LC-MS/MS spectra produced and matched by SEQUEST to the full V-region tryptic peptide GGNLLGIRPFDSWGQGTLVTVSSASTK (for measles) and MIGSSAWYPFDYWGQGTLVAVSSASTK (for mumps) contain heavy chain CDR3 (underlined) and their junction with the framework-4.

(C) Number of HCDR3 sequences identified from a total of 24,003 gamma chain sequences from subset A, 90,061 from B, 158,114 from D, and 28,351 from naive B cells that match the peptide sequences obtained in (B).

(D) Specificity of recombinant monoclonal antibody reconstituted from the VH and VL sequences from the BM subset D NGS data that aligned with VH and VL tryptic peptides HCDR3 AKMIGSSAWYPFDY and LCDR3 GTWDSSLGIVL from the mump-eluted fractions. Total anti-measles and mumps activities from the original serum are shown as controls.

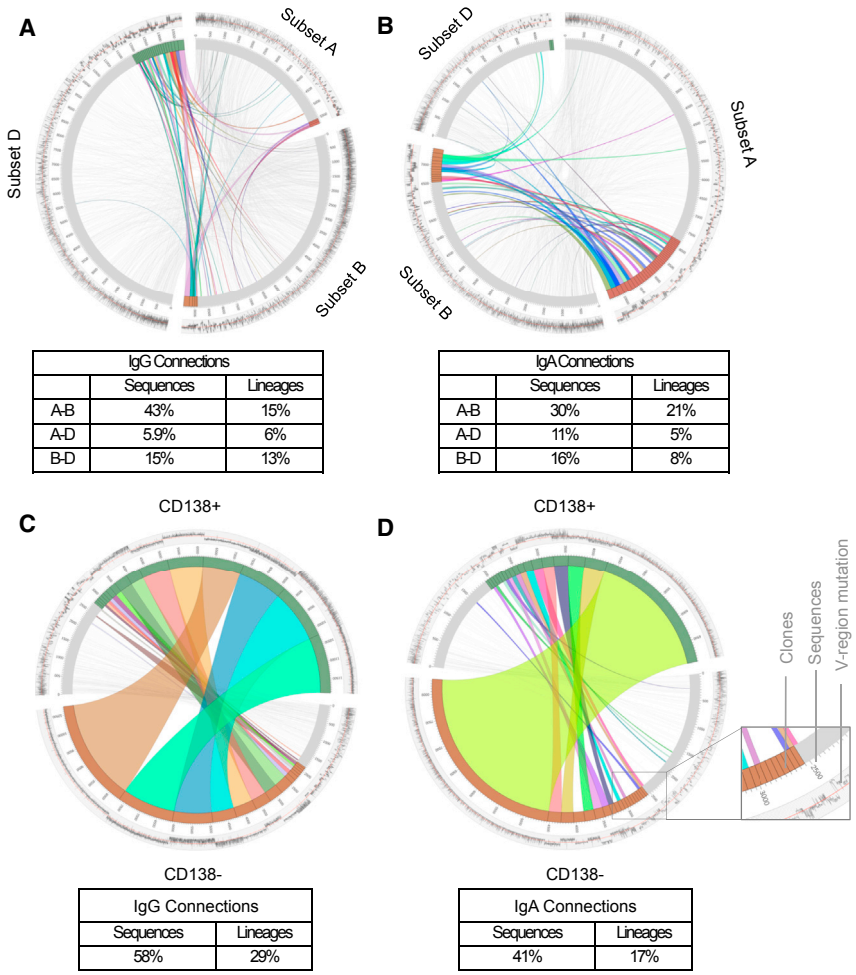

IgG Connections		
	Sequences	Lineages
A-B	43%	15%
A-D	5.9%	6%
B-D	15%	13%

IgA Connections		
	Sequences	Lineages
A-B	30%	21%
A-D	11%	5%
B-D	16%	8%

IgG Connections	
Sequences	Lineages
58%	29%

IgA Connections	
Sequences	Lineages
41%	17%

Figure 6. Connectivity of VH Repertoires of PC Subsets in the BM

Connectivity is shown with circos plots for (A) IgG and (B) IgA sequences for PC subsets A, B, and D in the BM of a 40-year-old adult at steady state. Connectivity is indicated for (C) IgG and (D) IgA sequences from CD138$^+$ and CD138$^-$ PB subsets in peripheral blood 7 days after tetanus vaccination (age 56 years old). The red line in the outer ring denotes the average number of mutations for each population and the gray trace represents the number of mutations found in each clone. The second track indicates the numbers of individual sequences. The divisions in the third track identify separate clonal populations. Clonal relationships are indicated by gray or colored lines and the thickness of the lines represents the number of clones related between populations. Colored lines in the middle represent relationships between clonotypes that consist of more than 50 sequences, and the gray lines denote relationships of clonotypes of fewer than 50 sequences. Boxes below show percent of sequences or clonotypes that are connected between the indicated PC/PB subsets in the BM or blood.

including a largely independent segment, whereas recently expanded peripheral PBs after acute antigen exposure are highly inter-related and are primarily comprised of a limited number of expanded clones.

Subset D Has a Distinct RNA Transcriptome with Genes Involved in Autophagy

To further understand the properties and mechanisms of survival of subset D as the LLPC compartment, we performed RNA sequencing in BM subsets A, B, and D at steady state in five separate healthy adults (mean ages 44 ± 12 years, 25 to 54 years). (Subset C was not collected due to variable BLIMP-1 staining or low numbers.) Gene expression was log-transformed and selected based on pairwise comparisons from 20,692 available genes for false discovery rate (FDR) < 0.00001 and absolute value of fold change >1.5. In the BM, 74, 768, and 154 genes were differentially expressed between subsets A and B, A and D, and B and D, respectively (Figures 7A and 7B). Initial IPA canonical pathway analysis identified several pathways important for BM survival including CD28 and mTOR signaling.

PCA analysis showed that subset D clearly segregated from subsets A and B following a pattern of sequential differentiation progressing from subset A to B to D along PC1 (Figure 7C). Of significant interest, genes involved in activation of autophagy, a process shown to be critical for the survival and function of mouse PCs (Pengo et al., 2013), were a major contributor to PCA separation of subset D relative to the other BM PC populations (differentially expressed genes involved in autophagy are listed in Figure S3).

To further explore autophagy activation, we performed LC3BII staining by confocal microscopy and enumerated autophagosomes by electron microscopy (EM). Punctate LC3BII is a well-established marker of activated autophagy resulting from conversion of the autophagy factor LC3BI (*ATG8*) to its phosphatidylethanolamine-conjugated form LC3BII, leading to its association with the autophagosome membrane. Punctuate LC3BII expression is unique to subset D (Figure 7D). In addition, EM also showed a higher frequency of autophagosomes in subset D (85% of all subset D PCs) compared to 50% in subset A or 55% in subset B PCs (Figures 7E and 7F). Combined, transcriptome analysis and microscopy results indicate that activated autophagy is a distinctive feature of subset D and identify this pathway as an important mechanism of survival of human LLPCs.

DISCUSSION

Acute recall immune responses generate short-lived proliferative plasmablasts that produce a transient burst of antigen-specific antibodies. Thereafter, pathogen-specific antibodies are sustained by resting, terminally differentiated PCs that in mouse models might survive for the life of the animal. Similarly, LLPCs have been proposed in humans to explain the persistence, in the absence of antigen-specific stimulation, of anti-microbial

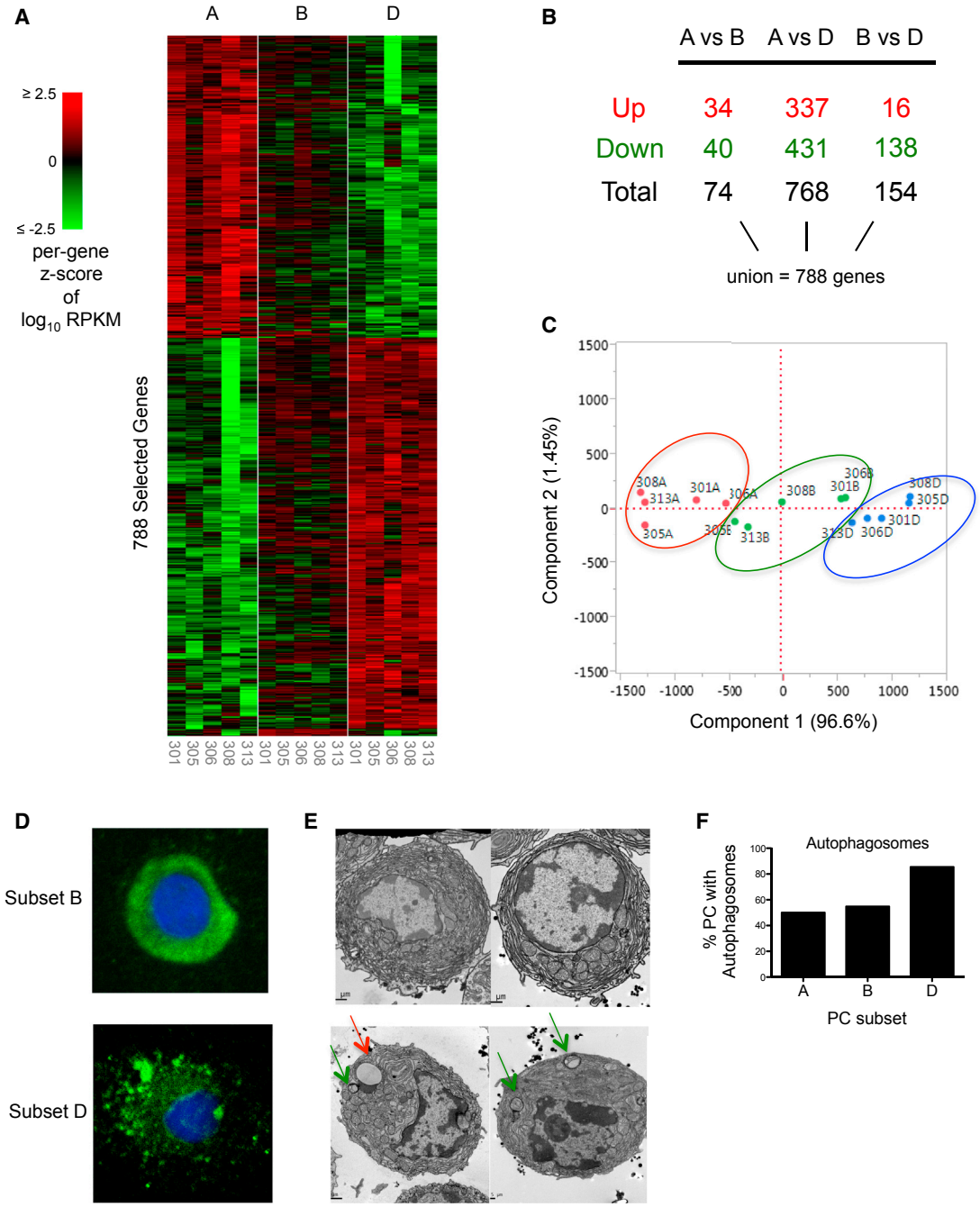

Figure 7. Transcriptome Analysis of PC Subsets and Upregulation of Autophagy Pathways

(A) Numbers of selected genes are shown from five BM aspirates sorted for subsets A, B, and D. Genes were selected based on pairwise comparisons from a total of 20,692 available genes. False discovery rates (FDR) were computed from p values as described by Storey (2002). Heat map shows per-gene z-score of log10-transformed, replicate-averaged data (zeros set to non-zero minimum of profiles). The selection criteria for a pairwise comparison were as follows: FDR < 0.00001, absolute value of fold change > 1.5, and the maximum group mean > −0.5 (roughly equivalent to non-log expression of 0.3).

(B) Numbers of genes differentially expressed between subsets A and B, A and D, and B and D. Directionality corresponds to the first group relative to the second. For example, "Up" in A versus B means A > B.

(C) Principal-component analysis for subsets A, B, and D based on 788 selected genes.

(D) LC3BII staining of subsets B and D by confocal microscopy.

(E) Electron microscopy of subsets A, B, and D. Red arrow shows lipid droplets, green arrows show autophagosomes (APs).

(F) Percentage of AP in BM PC subsets by EM (number of cells with APs/total cells) subset A: 11/22, subset B: 34/62, and subset D: 47/55.

antibodies with very long half-lives (10 to >3,000 years). However, direct proof for this mechanism and the actual identity of human LLPCs have remained elusive (González-García et al., 2006, 2008; Hargreaves et al., 2001; Liu et al., 2012; Mei et al., 2015; Odendahl et al., 2005; Qian et al., 2010; Radbruch et al., 2006), and alternative models, most notably the polyclonal bystander stimulation of memory cells, have been proposed to explain serological memory (Bernasconi et al., 2002). These critical gaps stem from the inability to determine the longevity of multiple PC subsets previously reported in the human BM and to ascribe the generation of long-lived antibodies to any singular population. Instead, location in the bone marrow, a resting state, and the expression of markers associated with ASC maturation (such as expression of CD138 and downregulation of HLA-DR or CD19) are frequently used as surrogate markers for LLPCs.

Here we identified in the human BM a population of $CD19^{-}$ $CD38^{hi}CD138^{+}$ cells (subset D) that unambiguously contains LLPCs. These cells have a distinctive morphology, express BLIMP-1, IRF4, and XBP-1, and are non-cycling. Critically, as determined by ELISPOT, subset D is the only population of cells to secrete antibodies specific for measles and mumps viruses more than 40 years after infection. Such a definitive link was demonstrated by exclusive matching of the serum anti-viral antibody proteome and the BCR repertoire expressed by subset D but not by any other BM PC compartment. These findings are validated by the demonstration that recombinant antibodies reconstructed from subset D sequences recapitulate the anti-viral specificity of the serum antibody fraction specific for the corresponding virus.

In contrast to subset D, other BM PC subsets produce antibodies against more recent antigens, such as influenza and tetanus, but not measles or mumps, thereby suggesting that they are relatively short-lived. Although these subsets share PC features, such as low expression of PAX5 and CD20 and high expression of BLIMP-1, XBP-1, and IRF4, other characteristics were indicative of a more short-lived phenotype. Thus, consistent with recent differentiation from B cells, significant fractions of subsets A–C retained sIg and MHC class II and expressed lower levels of CD27. Similarly, substantial Ki-67 expression in subsets A–C is in keeping with recent derivation from proliferating precursors.

The longevity of measles- and mumps-specific antibody responses is attributed to the intrinsic lifespans of LLPCs generated after viral infection. However, despite being generated by vaccination, the half-life of the tetanus-specific antibody response is remarkably long at 11 years (Amanna et al., 2007), compared to the much shorter half-life of antibody responses to polysaccharides (Kelly et al., 2006). Thus, it is perhaps not surprising that, under steady-state conditions, we find tetanus-specific PCs in the LLPC compartment. Nevertheless, the faster decay of anti-tetanus responses relative to anti-measles and -mumps responses demonstrates significant variability in the lifespan of LLPCs generated under different conditions.

Antibody responses to influenza vaccination also decline relatively quickly, although detectable serum titers can persist for 90 years (Yu et al., 2008), suggesting that both short-lived and long-lived PCs are generated. Consistent with this idea, we find influenza-specific PCs in subsets A and B as well as in subset D. Given that the influenza virus is constantly changing by yearly antigenic drift and the occasional shift in subtype (Palese and Shaw, 2007), it could be predicted that influenza-specific PCs in subset D will produce antibodies against temporally distant serotypes, whereas cells in subsets A, B, and even D will contain cells reactive with more contemporary serotypes. In addition, the presence of anti-influenza antibodies in LLPCs could represent responses to the conserved nucleoprotein antigens shared between influenza strains encountered decades apart (Kaminski and Lee, 2011). Differentiating between these possibilities will require comprehensive studies of the fine specificity of anti-influenza PCs.

LLPCs could derive from B cell precursors shared by other BM PC subsets through a progressive differentiation process in which phenotypic changes in the different PC subsets would reflect the age of the cells in each population, with the oldest cells progressively losing CD19 and surface Ig. This sequential differentiation model is supported by the progressive transcriptional separation of the different PC populations demonstrated by PCA, which would be consistent with sequential maturation of subset D from common precursors differentiating through stages A and B.

Alternatively, LLPCs could originate from separate precursors that would activate specific differentiation, homing, and/or survival programs that ultimately determine their longevity upon taking residence in the bone marrow microenvironment. Our current data cannot definitively distinguish between these models. Extended longitudinal studies after primary immunization with neoantigens will be required to clarify the ontogeny of human LLPCs.

Nevertheless, human LLPCs are distinguished from other BM PCs, including other $CD138^{+}$ cells, by several unique features that provide important mechanistic insights regarding their differentiation and survival programs. Thus, subset D cells include prominent cytoplasmic vacuoles representative of ongoing lysosomal autophagy, a process recently recognized as critical for PC homeostasis by regulating Ig secretion and optimizing energy metabolism and survival (Pengo et al., 2013). In keeping with this concept, the combination of transcriptional programs and microscopy analysis strongly point to active autophagy as a major mechanism of LLPC survival.

This study contributes the first high-throughput sequencing analysis of human BM PCs. NGS is a powerful means of testing the expected properties of a separate LLPCs. A central prediction for a distinct LLPC compartment is that, over a lifetime, it would progressively accumulate cells that have responded to a myriad of antigens. A corollary of this prediction is that in adults, a well-established LLPC would display a highly diversified repertoire, a property that is consistent with our results. Interestingly, repertoire analysis established the presence of two distinct components in subset D. We postulate that the larger component, which is uncoupled from other BM PC populations, represents steady-state LLPCs containing the historical record of B cell responses, a conclusion supported by the exclusive presence of mumps- and measles-specific PCs in subset D decades after antigen exposure. In contrast, a much smaller fraction of subset D is clonally connected with subsets A and B, a feature we interpret as indicative of new arrivals derived from more recent B cell responses. Newcomers into the D subset might eventually become bona fide LLPCs and contribute to the steady-state

fraction depending on their intrinsic longevity (Amanna and Slifka, 2010) and/or their ability to compete for survival niches. This model would also account for the presence of some Ki-67$^+$ cells in subset D, because these cells can be derived from recently dividing precursors (Cassese et al., 2003; Radbruch et al., 2006). Alternatively, the presence of a low frequency of Ki-67$^+$ cells in subset D could indicate that limited homeostatic proliferation might be important to maintain the LLPC pool, as shown for human memory cells (Macallan et al., 2005).

In summary, the identification of CD19$^-$CD38^{hi}CD138$^+$ cells in human BM as a bona fide LLPC compartment will enable investigators to understand the cellular source of different types of protective and pathogenic antibodies. It will also pave the way for a precise understanding of the molecular roadmaps underlying the differentiation and survival of this critical compartment. In turn, this knowledge will be central to our ability to maximize the generation of long-lived protective responses in microbial vaccination and prevent the accumulation of pathogenic PCs in autoimmune diseases and transplantation.

EXPERIMENTAL PROCEDURES

Subjects

Bone marrow aspirates were obtained from 35 healthy adults (age 22–70 years, mean 44 ± 13). Eleven of these subjects were older (age >40 years, range 43 to 70, mean 52 ± 8 years) and were recruited due to high serum titers of measles or mumps from history of natural infection with measles and mumps viruses during childhood. All adult subjects were vaccinated to influenza vaccination 1–11 months prior to BM aspirates. Blood and bone marrow aspirate was obtained from each patient and mononuclear cells were isolated by density gradient centrifugation. Blood for serum and BM were also obtained from one 64-year-old man for proteomics studies. For vaccinated and healthy asymptomatic adults, two healthy adult subjects (ages 27 and 56 years) were enrolled. Subjects received the tetanus toxoid vaccinations Td or combination Tdap as a part of routine medical care. PBMCs were isolated pre-vaccine and on days 6–7 for all vaccination subjects. All subjects in this study were recruited at the University of Rochester Medical Center or Emory University, and all studies were approved by the Institutional Review Boards at the University of Rochester Medical Center and Emory University.

VH Next-Generational Sequencing

Total cellular RNA was isolated from blood CD19$^+$CD138$^+$ and CD19$^+$CD138$^-$ PBs after tetanus vaccination BM PC subsets A, B, and D from three BM using the RNeasy Mini Kit (QIAGEN) by following the manufacturer's protocol. Approximately 400 pg of RNA was subjected to reverse transcription with the iScript RT kit (BioRad). Resulting cDNA products were included with 50 nM VH1-VH6-specific primers and 250 nM Ca-, Cm-, and Cg-specific primers in a 20 μl PCR reaction using High Fidelity Platinum PCR Supermix (Life Technologies) and amplified by 40 cycles. Nextera indices were added and products were sequenced on an Illumina MiSeq with a depth of approximately 300,000 sequences per sample. One BM sample was used as a control, 20,000 subset D cells were collected, RNA was isolated, and NGS was performed as described above. All sequences were aligned with IMGT.org/HighVquest (Alamyar et al., 2012). Sequences were then analyzed for V region mutations and clonality. All clonal assignments were based on matching V and J regions, matching CDR3 length, and 70% CDR3 homology. All sequences are plotted with Matlab or Circos visualization tools (Krzywinski et al., 2009).

Serum Proteomics

Measles- or mumps-specific polyclonal antibodies from one adult (age 64 years) were purified by affinity chromatography using a custom column consisting of measles or mumps antigens and fractions were eluted, verified for measles or mumps activity, then digested with chymotrypsin, pepsin, elastase, and trypsin and analyzed by the LC-MS/MS. MS/MS spectra were searched with SEQUEST against the V-region full peptides generated from the sequences provided by the NGS results of subsets A, B, and D and naive B cells. Top candidate V-region sequences including CDR3 peptides from measles and mumps antibodies were identified as previously described (Cheung et al., 2012; Sato et al., 2012).

Monoclonal Mumps-Specific Antibody Reconstruction

The top candidate gamma and kappa chains, containing HCDR3 AKMIGSSA WYPFDY and LCDR3 GTWDSSLGIVL, identified in subset D from the affinity-purified mumps-specific antibodies through the use of proteomics, were synthesized, cloned, and expressed in 293T cells. Specificity of the monoclonal antibody was tested by ELISA against measles and mumps antigens.

ACCESSION NUMBERS

The accession number for the NGS VH repertoire and RNA transcriptome dataset reported in this paper is SRA: SRP057017.

SUPPLEMENTAL INFORMATION

Supplemental Information includes three figures, one table, and Supplemental Experimental Procedures and can be found with this article online at http://dx.doi.org/10.1016/j.immuni.2015.06.016.

ACKNOWLEDGMENTS

The authors would like to thank Jennifer Scantlin, Claudine Nkurunziza, Deanna Maffett, and Julie Kozarsky for human subject recruitment. We also appreciate Edmund Waller, Jeremy Bechelli, Karen Rosell, and the Atlanta Clinical & Translational Science Institute (ACTSI) for their assistance with the bone marrow aspirates; Chelsea Cook, Flow Cytometry Core at URMC, and Wayne Harris at Emory University; and Jennifer Hom, Linda Kippner, and Melissa Kemp for assistance in preparation of the manuscript. This research was supported by NIH grants K23 AI67501, R21AI109601, R21AI094218, P01 A1078907, R37AI049660, and U01AI045969; Autoimmunity Center of Excellence grants ARRA:AI056390-06S2, HHSN266200500030C (N01-AI50029), AI078907, and AI049600; NIH/NCATS grants UL1 TR000454 and UO1 AI082196; and Oregon National Primate Research Center grants 8P51 OD011092-53, R01 AI097357, and U19 AI109962. F.E.-H.L. has research grants with Genentech and is the founder of MicroBplex. I.S. consults for Pfizer and Genentech and has research grants with Biogen and Takeda Pharmaceuticals. A.R.F. consults for AstraZeneca, Medimmune, Sanofi Pasteur, and Wyeth and has research grants from GSK and Sanofi Pasteur. E.E.W. has research grants from GSK and Sanofi Pasteur and consults for Astra Zeneca.

Received: August 16, 2014
Revised: January 16, 2015
Accepted: April 28, 2015
Published: July 14, 2015

REFERENCES

Ahuja, A., Anderson, S.M., Khalil, A., and Shlomchik, M.J. (2008). Maintenance of the plasma cell pool is independent of memory B cells. Proc. Natl. Acad. Sci. USA *105*, 4802–4807.

Alamyar, E., Giudicelli, V., Li, S., Duroux, P., and Lefranc, M.P. (2012). IMGT/HighV-QUEST: the IMGT(R) web portal for immunoglobulin (IG) or antibody and T cell receptor (TR) analysis from NGS high throughput and deep sequencing. Immunome Res. *8*, 26.

Amanna, I.J., and Slifka, M.K. (2010). Mechanisms that determine plasma cell lifespan and the duration of humoral immunity. Immunol. Rev. *236*, 125–138.

Amanna, I.J., Carlson, N.E., and Slifka, M.K. (2007). Duration of humoral immunity to common viral and vaccine antigens. N. Engl. J. Med. *357*, 1903–1915.

Avery, D.T., Ellyard, J.I., Mackay, F., Corcoran, L.M., Hodgkin, P.D., and Tangye, S.G. (2005). Increased expression of CD27 on activated human memory B cells correlates with their commitment to the plasma cell lineage. J. Immunol. *174*, 4034–4042.

Benson, M.J., Dillon, S.R., Castigli, E., Geha, R.S., Xu, S., Lam, K.P., and Noelle, R.J. (2008). Cutting edge: the dependence of plasma cells and independence of memory B cells on BAFF and APRIL. J. Immunol. *180*, 3655–3659.

Bernasconi, N.L., Traggiai, E., and Lanzavecchia, A. (2002). Maintenance of serological memory by polyclonal activation of human memory B cells. Science *298*, 2199–2202.

Cambridge, G., Leandro, M.J., Teodorescu, M., Manson, J., Rahman, A., Isenberg, D.A., and Edwards, J.C. (2006). B cell depletion therapy in systemic lupus erythematosus: effect on autoantibody and antimicrobial antibody profiles. Arthritis Rheum. *54*, 3612–3622.

Cassese, G., Arce, S., Hauser, A.E., Lehnert, K., Moewes, B., Mostarac, M., Muehlinghaus, G., Szyska, M., Radbruch, A., and Manz, R.A. (2003). Plasma cell survival is mediated by synergistic effects of cytokines and adhesion-dependent signals. J. Immunol. *171*, 1684–1690.

Cheung, W.C., Beausoleil, S.A., Zhang, X., Sato, S., Schieferl, S.M., Wieler, J.S., Beaudet, J.G., Ramenani, R.K., Popova, L., Comb, M.J., et al. (2012). A proteomics approach for the identification and cloning of monoclonal antibodies from serum. Nat. Biotechnol. *30*, 447–452.

Fairfax, K.A., Kallies, A., Nutt, S.L., and Tarlinton, D.M. (2008). Plasma cell development: from B-cell subsets to long-term survival niches. Semin. Immunol. *20*, 49–58.

González-García, I., Ocaña, E., Jiménez-Gómez, G., Campos-Caro, A., and Brieva, J.A. (2006). Immunization-induced perturbation of human blood plasma cell pool: progressive maturation, IL-6 responsiveness, and high PRDI-BF1/BLIMP1 expression are critical distinctions between antigen-specific and nonspecific plasma cells. J. Immunol. *176*, 4042–4050.

González-García, I., Rodríguez-Bayona, B., Mora-López, F., Campos-Caro, A., and Brieva, J.A. (2008). Increased survival is a selective feature of human circulating antigen-induced plasma cells synthesizing high-affinity antibodies. Blood *111*, 741–749.

Halliley, J.L., Kyu, S., Kobie, J.J., Walsh, E.E., Falsey, A.R., Randall, T.D., Treanor, J., Feng, C., Sanz, I., and Lee, F.E. (2010). Peak frequencies of circulating human influenza-specific antibody secreting cells correlate with serum antibody response after immunization. Vaccine *28*, 3582–3587.

Hargreaves, D.C., Hyman, P.L., Lu, T.T., Ngo, V.N., Bidgol, A., Suzuki, G., Zou, Y.R., Littman, D.R., and Cyster, J.G. (2001). A coordinated change in chemokine responsiveness guides plasma cell movements. J. Exp. Med. *194*, 45–56.

Hauser, A.E., Debes, G.F., Arce, S., Cassese, G., Hamann, A., Radbruch, A., and Manz, R.A. (2002). Chemotactic responsiveness toward ligands for CXCR3 and CXCR4 is regulated on plasma blasts during the time course of a memory immune response. J. Immunol. *169*, 1277–1282.

Hilbert, D.M., Kopf, M., Mock, B.A., Köhler, G., and Rudikoff, S. (1995). Interleukin 6 is essential for in vivo development of B lineage neoplasms. J. Exp. Med. *182*, 243–248.

Huggins, J., Pellegrin, T., Felgar, R.E., Wei, C., Brown, M., Zheng, B., Milner, E.C., Bernstein, S.H., Sanz, I., and Zand, M.S. (2007). CpG DNA activation and plasma-cell differentiation of CD27- naive human B cells. Blood *109*, 1611–1619.

Jourdan, M., Caraux, A., Caron, G., Robert, N., Fiol, G., Rème, T., Bolloré, K., Vendrell, J.P., Le Gallou, S., Mourcin, F., et al. (2011). Characterization of a transitional preplasmablast population in the process of human B cell to plasma cell differentiation. J. Immunol. *187*, 3931–3941.

Kaminski, D.A., and Lee, F.E. (2011). Antibodies against conserved antigens provide opportunities for reform in influenza vaccine design. Front. Immunol. *2*, 76.

Kelly, D.F., Snape, M.D., Clutterbuck, E.A., Green, S., Snowden, C., Diggle, L., Yu, L.M., Borkowski, A., Moxon, E.R., and Pollard, A.J. (2006). CRM197-conjugated serogroup C meningococcal capsular polysaccharide, but not the native polysaccharide, induces persistent antigen-specific memory B cells. Blood *108*, 2642–2647.

Krzywinski, M., Schein, J., Birol, I., Connors, J., Gascoyne, R., Horsman, D., Jones, S.J., and Marra, M.A. (2009). Circos: an information aesthetic for comparative genomics. Genome Res. *19*, 1639–1645.

Kyu, S.Y., Kobie, J., Yang, H., Zand, M.S., Topham, D.J., Quataert, S.A., Sanz, I., and Lee, F.E. (2009). Frequencies of human influenza-specific antibody secreting cells or plasmablasts post vaccination from fresh and frozen peripheral blood mononuclear cells. J. Immunol. Methods *340*, 42–47.

Lee, F.E., Halliley, J.L., Walsh, E.E., Moscatiello, A.P., Kmush, B.L., Falsey, A.R., Randall, T.D., Kaminiski, D.A., Miller, R.K., and Sanz, I. (2011). Circulating human antibody-secreting cells during vaccinations and respiratory viral infections are characterized by high specificity and lack of bystander effect. J. Immunol. *186*, 5514–5521.

Liu, D., Lin, P., Hu, Y., Zhou, Y., Tang, G., Powers, L., Medeiros, L.J., Jorgensen, J.L., and Wang, S.A. (2012). Immunophenotypic heterogeneity of normal plasma cells: comparison with minimal residual plasma cell myeloma. J. Clin. Pathol. *65*, 823–829.

Macallan, D.C., Wallace, D.L., Zhang, Y., Ghattas, H., Asquith, B., de Lara, C., Worth, A., Panayiotakopoulos, G., Griffin, G.E., Tough, D.F., and Beverley, P.C. (2005). B-cell kinetics in humans: rapid turnover of peripheral blood memory cells. Blood *105*, 3633–3640.

Manz, R.A., Thiel, A., and Radbruch, A. (1997). Lifetime of plasma cells in the bone marrow. Nature *388*, 133–134.

McMillan, R., Longmire, R.L., Yelenosky, R., Lang, J.E., Heath, V., and Craddock, C.G. (1972). Immunoglobulin synthesis by human lymphoid tissues: normal bone marrow as a major site of IgG production. J. Immunol. *109*, 1386–1394.

Medina, F., Segundo, C., Campos-Caro, A., González-García, I., and Brieva, J.A. (2002). The heterogeneity shown by human plasma cells from tonsil, blood, and bone marrow reveals graded stages of increasing maturity, but local profiles of adhesion molecule expression. Blood *99*, 2154–2161.

Mei, H.E., Wirries, I., Frölich, D., Brisslert, M., Giesecke, C., Grün, J.R., Alexander, T., Schmidt, S., Luda, K., Kühl, A.A., et al. (2015). A unique population of IgG-expressing plasma cells lacking CD19 is enriched in human bone marrow. Blood *125*, 1739–1748.

Miller, F.R. (1931). The induced development and histogenesis of plasma cells. J. Exp. Med. *54*, 333–347.

Morell, A., Terry, W.D., and Waldmann, T.A. (1970). Metabolic properties of IgG subclasses in man. J. Clin. Invest. *49*, 673–680.

Nie, Y., Waite, J., Brewer, F., Sunshine, M.J., Littman, D.R., and Zou, Y.R. (2004). The role of CXCR4 in maintaining peripheral B cell compartments and humoral immunity. J. Exp. Med. *200*, 1145–1156.

Odendahl, M., Mei, H., Hoyer, B.F., Jacobi, A.M., Hansen, A., Muehlinghaus, G., Berek, C., Hiepe, F., Manz, R., Radbruch, A., and Dörner, T. (2005). Generation of migratory antigen-specific plasma blasts and mobilization of resident plasma cells in a secondary immune response. Blood *105*, 1614–1621.

Oracki, S.A., Walker, J.A., Hibbs, M.L., Corcoran, L.M., and Tarlinton, D.M. (2010). Plasma cell development and survival. Immunol. Rev. *237*, 140–159.

Palese, P.S., and Shaw, M.L. (2007). Orthomyxoviridae: the viruses and their replication. In Fields Virology, D.H. Knipe and P.M. Howley, eds. (Philadelphia: Lippincott Williams& Wilkins), pp. 1647–1689.

Pengo, N., Scolari, M., Oliva, L., Milan, E., Mainoldi, F., Raimondi, A., Fagioli, C., Merlini, A., Mariani, E., Pasqualetto, E., et al. (2013). Plasma cells require autophagy for sustainable immunoglobulin production. Nat. Immunol. *14*, 298–305.

Qian, Y., Wei, C., Eun-Hyung Lee, F., Campbell, J., Halliley, J., Lee, J.A., Cai, J., Kong, Y.M., Sadat, E., Thomson, E., et al. (2010). Elucidation of seventeen human peripheral blood B-cell subsets and quantification of the tetanus response using a density-based method for the automated identification of cell populations in multidimensional flow cytometry data. Cytometry B Clin. Cytom. *78* (*Suppl 1*), S69–S82.

Radbruch, A., Muehlinghaus, G., Luger, E.O., Inamine, A., Smith, K.G., Dörner, T., and Hiepe, F. (2006). Competence and competition: the challenge of becoming a long-lived plasma cell. Nat. Rev. Immunol. *6*, 741–750.

Rawstron, A.C., Davies, F.E., DasGupta, R., Ashcroft, A.J., Patmore, R., Drayson, M.T., Owen, R.G., Jack, A.S., Child, J.A., and Morgan, G.J. (2002). Flow cytometric disease monitoring in multiple myeloma: the relationship

between normal and neoplastic plasma cells predicts outcome after transplantation. Blood *100*, 3095–3100.

Rozanski, C.H., Arens, R., Carlson, L.M., Nair, J., Boise, L.H., Chanan-Khan, A.A., Schoenberger, S.P., and Lee, K.P. (2011). Sustained antibody responses depend on CD28 function in bone marrow-resident plasma cells. J. Exp. Med. *208*, 1435–1446.

Sato, S., Beausoleil, S.A., Popova, L., Beaudet, J.G., Ramenani, R.K., Zhang, X., Wieler, J.S., Schieferl, S.M., Cheung, W.C., and Polakiewicz, R.D. (2012). Proteomics-directed cloning of circulating antiviral human monoclonal antibodies. Nat. Biotechnol. *30*, 1039–1043.

Skowronski, D.M., Tweed, S.A., and De Serres, G. (2008). Rapid decline of influenza vaccine-induced antibody in the elderly: is it real, or is it relevant? J. Infect. Dis. *197*, 490–502.

Slifka, M.K., and Ahmed, R. (1998). Long-lived plasma cells: a mechanism for maintaining persistent antibody production. Curr. Opin. Immunol. *10*, 252–258.

Storey, J.D. (2002). A direct approach to false discovery rates. J. R. Stat. Soc., B *64*, 479–498.

Tourigny, M.R., Ursini-Siegel, J., Lee, H., Toellner, K.M., Cunningham, A.F., Franklin, D.S., Ely, S., Chen, M., Qin, X.F., Xiong, Y., et al. (2002). CDK inhibitor p18(INK4c) is required for the generation of functional plasma cells. Immunity *17*, 179–189.

Turner, C.A., Jr., Mack, D.H., and Davis, M.M. (1994). Blimp-1, a novel zinc finger-containing protein that can drive the maturation of B lymphocytes into immunoglobulin-secreting cells. Cell *77*, 297–306.

Wrammert, J., Smith, K., Miller, J., Langley, W.A., Kokko, K., Larsen, C., Zheng, N.Y., Mays, I., Garman, L., Helms, C., et al. (2008). Rapid cloning of high-affinity human monoclonal antibodies against influenza virus. Nature *453*, 667–671.

Xiang, Z., Cutler, A.J., Brownlie, R.J., Fairfax, K., Lawlor, K.E., Severinson, E., Walker, E.U., Manz, R.A., Tarlinton, D.M., and Smith, K.G. (2007). FcgammaRIIb controls bone marrow plasma cell persistence and apoptosis. Nat. Immunol. *8*, 419–429.

Yu, X., Tsibane, T., McGraw, P.A., House, F.S., Keefer, C.J., Hicar, M.D., Tumpey, T.M., Pappas, C., Perrone, L.A., Martinez, O., et al. (2008). Neutralizing antibodies derived from the B cells of 1918 influenza pandemic survivors. Nature *455*, 532–536.